

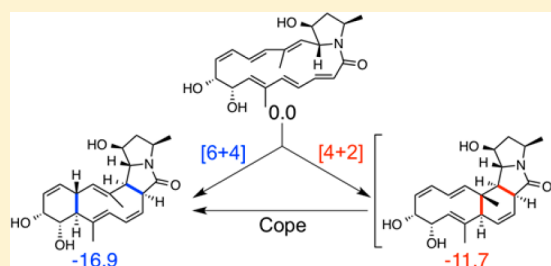
# Transannular [6 + 4] and Ambimodal Cycloaddition in the Biosynthesis of Heronamide A

Peiyuan Yu,<sup>†</sup> Ashay Patel,<sup>†</sup> and K. N. Houk<sup>\*,†,‡</sup>

<sup>†</sup>Department of Chemistry and Biochemistry, <sup>‡</sup>Department of Chemical and Biomolecular Engineering, University of California, Los Angeles, California 90095, United States

## Supporting Information

**ABSTRACT:** The transannular [6 + 4] cycloaddition proposed as a step in the biosynthesis of heronamide A has been modeled using density functional theory. The proposed cycloaddition is highly stereoselective, affording a single product. The reaction proceeds through an ambimodal transition state that directly leads to a [4 + 2] adduct in addition to the observed [6 + 4] adduct. Interconversion of these adducts is possible via a facile Cope rearrangement. The [6 + 4] adduct is thermodynamically more stable than the [4 + 2] adduct by 5.2 kcal mol<sup>-1</sup> due to a combination of the ring and steric strain in the [4 + 2] product. The results strongly support the plausibility of the proposed transannular [6 + 4] cycloaddition in the biogenesis of heronamide A and may provide insights to designing substrates that selectively undergo [6 + 4] cycloaddition to form unbridged 10-membered rings.



## INTRODUCTION

Woodward and Hoffmann first predicted that thermal [6 + 4] cycloadditions were allowed pericyclic transformations in 1965, when no cycloadditions involving 10 electrons were known.<sup>1</sup> The search for such a reaction was the subject of the Ph.D. research of coauthor K. N. Houk in the Woodward group.<sup>2</sup> In 1966, the first observations of a [6 + 4] cycloadduct occurred independently in the laboratories of Cookson<sup>3</sup> and Ito.<sup>4</sup> Now it seems that nature enlisted this reaction in biosynthesis long before chemists discovered it. In the nearly 5 decades since the Cookson–Ito reports, the mechanism and synthetic utility of this reaction have been studied widely.<sup>5–13</sup> Despite these studies, the utility of [6 + 4] cycloaddition has remained rather limited, especially in comparison to the ubiquitous [4 + 2] Diels–Alder reaction. The 6 $\pi$ -electron cycloaddends utilized in [6 + 4] cycloadditions have generally been limited to cyclic trienes such as cycloheptatrienes, fulvenes, and tropones. As a result, the cycloadducts resulting from these reactions all contain bridged 10-membered ring structures, and the formation of unbridged 10-membered rings by [6 + 4] cycloadditions remains unrealized. Alder et al. have modeled computationally a number of [6 + 4] cycloadditions to explain the origins of this limitation and to propose substrates that may undergo the desired cycloaddition.<sup>14</sup> They find that often a competing Diels–Alder cycloaddition is more facile, and in many of the cases where the [6 + 4] adduct is predicted to form, it can rapidly rearrange via a Cope rearrangement to yield the more stable [4 + 2] adduct. The biosynthesis of heronamide A suggests that nature has long solved the synthetic challenge of constructing unbridged 10-membered rings by [6 + 4] cycloaddition.

In 2010, Capon et al. isolated a new 20-membered polyene macrolactam, heronamide C (**1**), from fermentations of a marine-derived *Streptomyces* sp. (CMB-M0406), along with heronamide A (**2**) and heronamide B, both putatively derived from **1**.<sup>15</sup> After initial misassignment of the structures of these heronamides, spectroscopic<sup>16</sup> and synthetic<sup>17</sup> studies determined that the heronamides feature conserved stereochemistry, in support of the notions these species may be formed via a common biosynthetic pathway. Sugiyama and co-workers reported further proof of this when they demonstrated that **1** could spontaneously convert into **2** in DMSO.<sup>18</sup> Recently, Zhang et al. reported that heronamides D–F, which possess a two-carbon-shorter side chain compared with that of heronamides A–C, exhibit similar biosynthetic relationship.<sup>19</sup>

As shown in Scheme 1, the biosynthetic pathway proposed by Capon involves the site-selective oxidation of **1** to form epoxide **3**. Polyenes are known to be air-oxidized to afford epoxide derivatives spontaneously<sup>20</sup> or enzymatically.<sup>21</sup> The subsequent epoxide ring opening of **3** via S<sub>N</sub>2 attack of the amide nitrogen to form **4** is also likely to be feasible because of proximity and strain release.<sup>22</sup> The last step of the proposed pathway is an unprecedented transformation in which an unbridged 10-membered ring is constructed via a transannular [6 + 4] cycloaddition. We have explored this step using DFT computations.

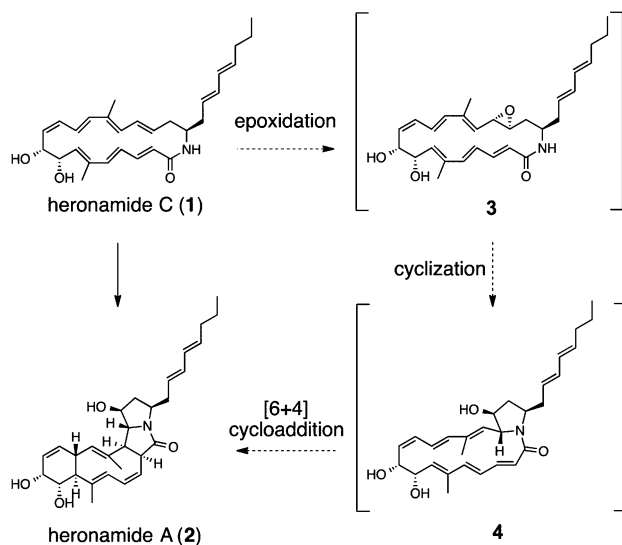
## COMPUTATIONAL METHODS

All density functional theory computations were performed using Gaussian09.<sup>23</sup> Geometry optimizations and subsequent frequency

Received: June 26, 2015

Published: October 5, 2015

### Scheme 1. Revised Structures of Heronamide C (1) and Heronamide A (2) and the Proposed Biosynthetic Relationship between Them



calculations were performed at the B3LYP/6-31G(d) level of theory,<sup>24</sup> both with and without Grimme's D3 empirical dispersion correction.<sup>25</sup> The empirical dispersion correction was found to have little effect on both the geometries and energies of stationary points; therefore, we have elected to report structures optimized at the B3LYP/6-31G(d) model chemistry. Normal vibrational mode analysis confirmed that optimized structures were minima or transition states. Zero-point vibrational energy (ZPE) and thermal corrections were calculated using unscaled B3LYP/6-31G(d) frequencies. Truhlar's quasiharmonic correction was used to compute molecular entropies to reduce error caused by the breakdown of the harmonic oscillator approximation, by setting all positive frequencies that are less than 100  $\text{cm}^{-1}$  to 100  $\text{cm}^{-1}$ .<sup>26</sup> Since the M06-2X method<sup>27</sup> has been shown to yield more accurate energetics for cycloaddition reactions,<sup>28</sup> M06-2X/6-311+G(d,p) single-point energies were computed on the B3LYP-optimized structures. For the model reaction, solvent effects were evaluated with the CPCM polarizable conductor model.<sup>29</sup> Reported energies are Gibbs free energies determined by summing these single-point electronic energies and ZPE and thermal corrections determined using B3LYP/6-31G(d). All 3D rendering of stationary points were generated using CYLview,<sup>30</sup> GaussView<sup>31</sup> and Avogadro<sup>32</sup> were used to construct the structures used in our computations.

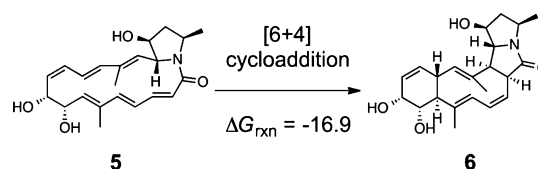
Conformational searches of the ground-state structures for all reactants, intermediates, and products were performed using the MMFF force field. A low mode/Monte Carlo (LMMC) search protocol optimized for sampling of macrocycles available in MacroModel 9.9 was performed.<sup>33</sup> Up to 50 lowest-energy structures in each case were then used as starting points for DFT optimization using the B3LYP/6-31G(d) level of theory.

## RESULTS AND DISCUSSION

**Model Reaction, Transition Structure, and Free Energy Diagram.** To reduce the time required for individual computation and to reduce the number of conformers that need to be sampled, we modeled the [6 + 4] cycloaddition of a truncated substrate, in which the octa-2,4-dien-1-yl side chain of heronamide A (and related compounds) was replaced with a methyl group.

Scheme 2 shows the [6 + 4] cycloaddition of model substrate 5. The reaction is computed to be exergonic by 16.9  $\text{kcal mol}^{-1}$ . To investigate the stereoselectivity of the reaction, 12 different transition states were located (see Supporting Information), with the lowest energy one shown in Figure 1 (TS-1,  $\Delta G^\ddagger =$

### Scheme 2. Model Reaction Scheme and Computed Reaction Free Energy<sup>a</sup>



<sup>a</sup>Energies reported are M06-2X/6-311+G(d,p)//B3LYP/6-31G(d) free energies in  $\text{kcal mol}^{-1}$ .

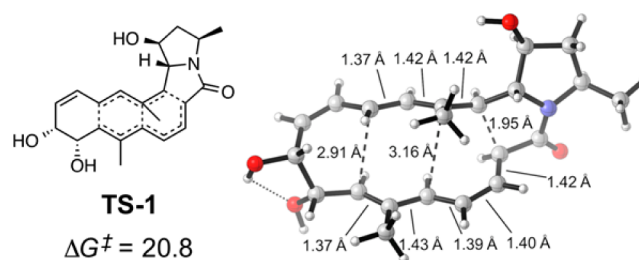


**Figure 1.** B3LYP/6-31G(d)-optimized transition structure for the ambimodal cycloaddition of 5. Energies reported are M06-2X/6-311+G(d,p)//B3LYP/6-31G(d) free energies in  $\text{kcal mol}^{-1}$ .

20.8  $\text{kcal mol}^{-1}$ ). The energies of the transition states leading to alternative products range from 23.3 to 40.4  $\text{kcal mol}^{-1}$ . The energy difference between TS-1 and the second lowest energy transition state is 2.5  $\text{kcal mol}^{-1}$ . This is in agreement with the experimental finding that 2 is formed exclusively. We also located a second transition state involving formation of only one bond, leading to a diradical intermediate. However, it is about 10  $\text{kcal mol}^{-1}$  higher in energy than TS-1. The activation free energy for this nonenzymatic reaction is 20.8  $\text{kcal mol}^{-1}$ . At 298 K, the reaction has a computed half-life ( $t_{1/2}$ ) of about 3 min. In comparison, the experimentally observed transformation of 1 to 2 takes days.<sup>18</sup> Therefore, it is unlikely that intermediate 4 could be observed prior to cycloaddition, and an earlier biosynthetic step is probably rate limiting.

As shown in Figure 1, TS-1 is highly asynchronous; the shortest partially formed  $\sigma$  bond has a forming bond length of 1.95 Å, and the second partially formed  $\sigma$  bond has a forming bond length of 2.91 Å. TS-1 has a third partially formed  $\sigma$  bond with a forming bond length of 3.16 Å, which corresponds to one of the two bonds that are formed by a [4 + 2] cycloaddition of 5. Although we made many attempts, we were not able to locate separate TS structures for this [4 + 2] cycloaddition. The [6 + 4] and [4 + 2] pathways are merged at TS-1. Such a transition state is described as ambimodal, as it leads directly to multiple products.<sup>34</sup> The [6 + 4]/[4 + 2] ambimodal transition state is bis-pericyclic in nature, with two sets of stabilizing cyclic aromatic orbital interactions.<sup>35</sup>

Figure 2a shows the free energy diagram of the ambimodal cycloaddition of 5. A valley-ridge inflection (VRI) point might exist along this pathway, where the potential energy surface (PES) bifurcates, leading to two distinct adducts: the observed [6 + 4] adduct 6 and a [4 + 2] adduct 7. The exact definition of a VRI point has been debated in the literature.<sup>36</sup> A more general concept, the so-called "valley-ridge transition (VRT) point", has been proposed recently.<sup>37</sup> The VRT point can be located unequivocally along the intrinsic reaction coordinate (IRC) of reactions that involve bifurcations.<sup>38</sup> Figure 2b shows the plot of energies of points along the forward IRC. To locate

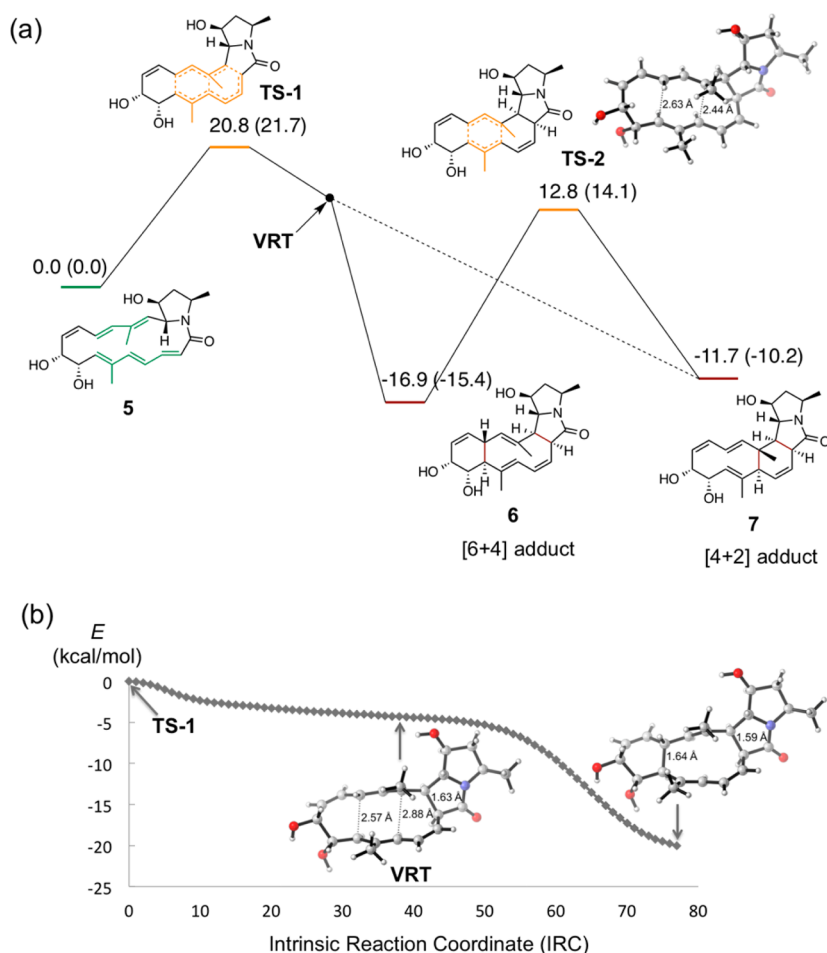


**Figure 2.** (a) Free energy diagram of the cycloaddition of macrolactam **5** featuring an ambimodal TS-1 that leads to the [6 + 4] and [4 + 2] adducts **6** and **7**, respectively. **7** can convert to **6** through Cope rearrangement via TS-2. Energies reported are M06-2X/6-311+G(d,p)//B3LYP/6-31G(d) free energies in kcal mol<sup>-1</sup>. Solvation has only a minor effect on the barriers of reaction and does not affect the relative stability of the two cycloadducts. Energies in parentheses are CPCM(Water)-M06-2X/6-311+G(d,p)//B3LYP/6-31G(d) free energies in kcal mol<sup>-1</sup>. (b) Plot of energies (B3LYP/6-31G(d)) versus points along the computed forward IRC starts from TS-1.

approximately the VRT point, we took every point along the IRC and computed the projected frequencies for vibrations perpendicular to the path. After the point indicated as VRT in Figure 2b, one imaginary frequency is found at each point. In other words, the valley becomes a ridge after this point. The product distribution of reactions occurring on bifurcating surfaces cannot be determined solely by transition state theory. Instead, the shape of the PES and resulting dynamical effects will play an important role.<sup>39</sup> For the reaction of **5**, the [4 + 2] adduct **7** is calculated to be 5.2 kcal mol<sup>-1</sup> less stable than the [6 + 4] adduct **6**. A possible Cope rearrangement reaction could convert **7** into **6**. Indeed, we located the Cope rearrangement transition state TS-2. It has a barrier of 24.5 kcal mol<sup>-1</sup>. Therefore, starting from substrate **5**, the [4 + 2] intermediate **7** should be observable, but it will convert to the more stable [6 + 4] adduct at room temperature. The IRC leads to a conformer of **6** (shown in Figure 2b, the last point on the IRC, where the cyclohexene ring adopts a boat conformation). This is in agreement with the behavior of most unsymmetrical bifurcating potential energy surfaces, where the calculated minimum energy path (MEP) leads to only one product.<sup>35,36,39</sup> In contrast, for symmetrical bifurcating PES such as the *endo* dimerization of cyclopentadiene,<sup>35a</sup> the MEP leads to the second TS. To provide further evidence for

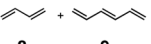
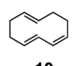
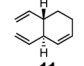
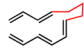
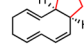
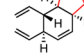
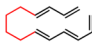
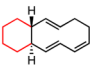
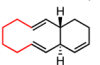
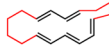
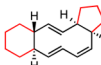
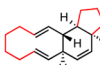
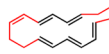
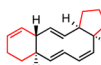
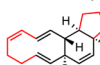
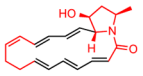
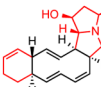
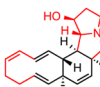
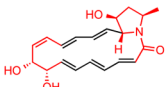
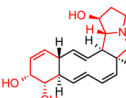
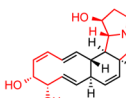
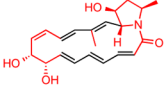
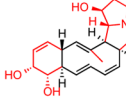
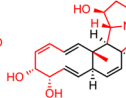
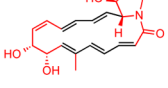
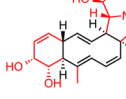
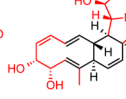
the connection between TS-1 and the unobserved [4 + 2] product **7** without undertaking dynamic trajectory studies for such a large system, we designed a truncated model substrate **5t**, for which the [6 + 4] and [4 + 2] products are the same in energy and the PES after the VRT point is symmetrical.<sup>40</sup> Indeed, the IRC that follows the ambimodal cycloaddition TS does lead to the Cope TS: a hallmark of symmetrical bifurcating PES.

Unlike the transannular cycloaddition of **5**, for which the [6 + 4] adduct **6** is more stable than the [4 + 2] adduct **7**, the ambimodal cycloaddition of 1,3,5-hexatriene and 1,3-butadiene yields the [4 + 2] adduct when under thermodynamic control.<sup>14</sup> To understand influence of substitution of the cycloaddends on the equilibrium between **6** and **7**, we modeled the cycloaddition of a series of model substrates. The results are summarized below.

#### Effects of Tethers on the Barrier of Reaction and Relative Stability of the [6 + 4] and [4 + 2] Cycloadducts.

Table 1 shows the computed reaction barriers and relative stability of adducts formed by the ambimodal cycloadditions of different substrates. These model substrates were chosen to interrogate the role of tethers and substituents on the reaction barriers and relative stability of the cycloadducts. For the cycloaddition of unsubstituted butadiene **8** and hexatriene **9**,

**Table 1. Effects of Tethers and Substituents on the Reaction Barriers and the Relative Stability of the [6 + 4] and [4 + 2] Cycloadducts<sup>a</sup>**

substrate(s)	TS <sub>[6+4]/[4+2]</sub>	[6+4] adduct	[4+2] adduct
 8 + 9	TS-3 32.7	 10 -12.2	 11 -18.7 (-6.4)
 12	TS-4 28.4	 13 -14.0	 14 -20.0 (-6.0)
 15	TS-5 26.6	 16 -19.3	 17 -18.1 (1.2)
 18	TS-6 24.8	 19 -18.2	 20 -17.0 (1.2)
 21	TS-7 25.9	 22 -11.2	 23 -10.9 (0.3)
 24	TS-8 19.8	 25 -16.3	 26 -15.5 (0.8)
 27	TS-9 20.7	 28 -16.9	 29 -15.4 (1.4)
 30	TS-10 19.9	 31 -15.2	 32 -13.7 (1.5)
 33	TS-11 21.3	 34 -17.9	 35 -16.2 (1.7)

<sup>a</sup>Energies reported are M06-2X/6-311+G(d,p)//B3LYP/6-31G(d) free energies in kcal mol<sup>-1</sup>. (Energies in parentheses are the difference between the two adducts.)

the [6 + 4] adduct **10** is less stable than the [4 + 2] adduct **11** by 6.4 kcal mol<sup>-1</sup> due to the strain of the medium-sized ring. The reaction barrier decreases by 4.3 kcal mol<sup>-1</sup> when the reaction changes from intermolecular to intramolecular. The three-carbon tether connected to C-9 and C-10 (**13**, shown in red) has little effect on the instability of the 10-membered ring relative to the six-membered isomer. However, when a four-carbon tether is added at the C-5 and C-6 positions of the 10-membered ring, the relative stability of the two adducts is reversed. The [6 + 4] adduct **16** is now more stable than the [4 + 2] adduct **17**. Because of the four-carbon tether, both adducts contain strained 10-membered rings. The small preference (1.2 kcal mol<sup>-1</sup>) for **16** is likely due to the alkene conjugation, which

is not present in **17**. An additional three-membered tether at the C-9 and C-10 positions has no effect on the relative stability of **19** and **20** (1.2 kcal mol<sup>-1</sup>). An additional double bond in the four-carbon tether slightly stabilizes the [4 + 2] adduct (the difference becomes 0.3 kcal mol<sup>-1</sup>), probably due to additional alkene conjugation in **23** compared to **20**. When the full amide tether is added (**24**), the reaction barrier drops significantly by 6.1 kcal mol<sup>-1</sup>. This is not totally unexpected, because of the electron-withdrawing nature of the carbonyl group. The same small preference for the [6 + 4] product is preserved (1.4 kcal mol<sup>-1</sup>) when the full tethers are added (**27**). Thus, the four-carbon tether linking C-5 and C-6 destabilizes the [4 + 2] adduct by introducing a strained medium-sized ring in this product, whereas the amide tether is responsible for lowering the barrier of this reaction. On the basis of these results, the tether effects are only partially responsible for the large energy difference between **6** and **7** (5.2 kcal mol<sup>-1</sup>): a 10:1 mixture of these adducts would be expected at room temperature (based on the energy difference between **28** and **29**).

**Effects of Methyl Substituents on the Relative Stability of the [6 + 4] and [4 + 2] Cycloadducts.** We next probed the effects of methyl substituents on **6** and **7**. As shown in [Figure 3](#), all methyl groups on the 10-membered rings

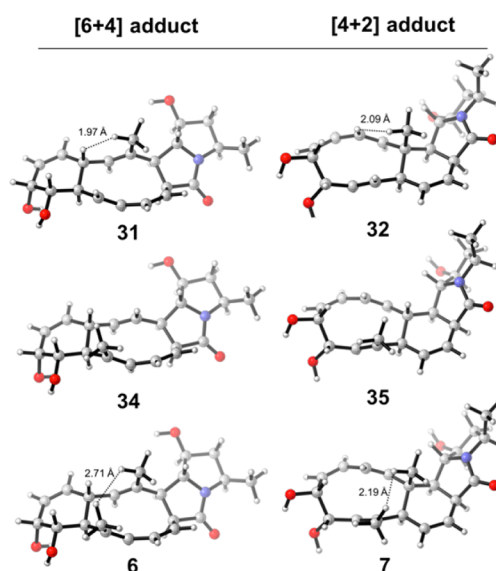


**Figure 3.** B3LYP/6-31G(d)-optimized [6+4] adducts **31**, **34**, **6**, and [4+2] adducts **32**, **35**, **7**.

adopt pseudoaxial orientations. A single methyl group at the C-4 or C-8 position has little effect on the equilibrium between the [6 + 4] and [4 + 2] adducts ([Table 1](#)). The energy differences between **31** and **32** (1.5 kcal mol<sup>-1</sup>) as well as **34** and **35** (1.7 kcal mol<sup>-1</sup>) are virtually identical to that of **28** and **29** (1.4 kcal mol<sup>-1</sup>). For **31**, the stabilizing effect of a methyl group on the double bond is likely canceled by increased allylic 1,3-strain<sup>41</sup> in **31** as compared to **32** ([Figure 3](#), 1.97 vs 2.09 Å). However, when both methyl substituents are present on the cycloaddends, as in **5**, the resulting [4 + 2] adduct **7** is now less stable than the [6 + 4] adduct **6** by 5.2 kcal mol<sup>-1</sup>. The hydrogen atom distance indicated in **7** is 2.19 Å, whereas the two methyl groups are separated far from each other in **6**. The 3.5–3.8 kcal mol<sup>-1</sup> increase in relative energies compared with analogues of monomethyl or lacking methyl is the result of steric interactions between the two methyl groups in **7**. For

comparison, the 1,3-diaxial methyl–methyl interactions measured in a substituted chair cyclohexane are destabilizing by 3.7 kcal mol<sup>-1</sup>,<sup>42</sup> and the methyl–methyl repulsion is similar in 7.

## CONCLUSIONS

The unprecedented transannular [6 + 4] cycloaddition in a proposed biosynthetic pathway of heronamide A has been investigated by density functional theory computations. Calculations indicate that the [6 + 4] cycloaddition is stereoselective and proceeds through an ambimodal transition state that can lead to both the observed [6 + 4] and unobserved [4 + 2] products. However, the [4 + 2] product is less stable than the [6 + 4] product by 5.2 kcal mol<sup>-1</sup>, due to a combination of tether effects and steric repulsions between two methyl groups in the [4 + 2] product. The results strongly support the plausibility of the biosynthetic [6 + 4] cycloaddition and may lead to the development of new synthetic strategies for using transannular [6 + 4] cycloaddition to construct polycyclic scaffolds featuring unbridged 10-membered rings.

## ASSOCIATED CONTENT

### Supporting Information

The Supporting Information is available free of charge on the ACS Publications website at DOI: 10.1021/jacs.5b06656.

Additional computational results, Cartesian coordinates, and energies of all stationary points (PDF)

## AUTHOR INFORMATION

### Corresponding Author

\*houk@chem.ucla.edu

### Notes

The authors declare no competing financial interest.

## ACKNOWLEDGMENTS

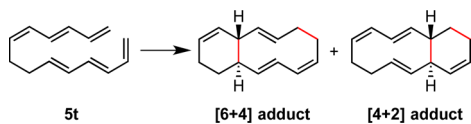
We are grateful to the National Science Foundation (CHE-1361104) for financial support of this research and to Professor B. Andes Hess Jr. for helpful comments. P.Y. acknowledges UCLA for its support. A.P. acknowledges the CBI and UCLA for their support. Calculations were performed on the Hoffman2 cluster at UCLA and the Extreme Science and Engineering Discovery Environment (XSEDE), which is supported by the NSF (OCI-1053575).

## REFERENCES

- (1) Hoffmann, R.; Woodward, R. B. *J. Am. Chem. Soc.* **1965**, *87*, 2046.
- (2) (a) Houk, K. N.; Woodward, R. B. *J. Am. Chem. Soc.* **1970**, *92*, 4143. (b) Houk, K. N.; Woodward, R. B. *J. Am. Chem. Soc.* **1970**, *92*, 4145.
- (3) Cookson, R. C.; Drake, B. V.; Hudec, J.; Morrison, A. *Chem. Commun.* **1966**, 15.
- (4) Ito, S.; Fujise, Y.; Okuda, T.; Inoue, Y. *Bull. Chem. Soc. Jpn.* **1966**, *39*, 1351.
- (5) Houk, K. N.; Luskus, L. J.; Bhacca, N. S. *J. Am. Chem. Soc.* **1970**, *92*, 6392.
- (6) Sasaki, T.; Kanematsu, K.; Iizuka, K. *J. Org. Chem.* **1976**, *41*, 1105.
- (7) Mukherjee, D.; Watts, C. R.; Houk, K. N. *J. Org. Chem.* **1978**, *43*, 817.
- (8) Garst, M. E.; Roberts, V. A.; Houk, K. N.; Rondan, N. G. *J. Am. Chem. Soc.* **1984**, *106*, 3882.
- (9) Funk, R. L.; Bolton, G. L. *J. Am. Chem. Soc.* **1986**, *108*, 4655.
- (10) Rigby, J. H.; Moore, T. L.; Rege, S. *J. Org. Chem.* **1986**, *51*, 2398.

- (11) Rigby, J. H.; Ateeq, H. S.; Charles, N. R.; Cuisiat, S. V.; Ferguson, M. D.; Henshilwood, J. A.; Krueger, A. C.; Ogbu, C. O.; Short, K. M.; Heeg, M. J. *J. Am. Chem. Soc.* **1993**, *115*, 1382.
- (12) Isakovic, L.; Ashenurst, J. A.; Gleason, J. L. *Org. Lett.* **2001**, *3*, 4189.
- (13) Hong, B.-C.; Jiang, Y.-F.; Kumar, E. S. *Bioorg. Med. Chem. Lett.* **2001**, *11*, 1981.
- (14) Alder, R. W.; Harvey, J. N.; Lloyd-Jones, G. C.; Oliva, J. M. *J. Am. Chem. Soc.* **2010**, *132*, 8325.
- (15) Raju, R.; Piggott, A. M.; Conte, M. M.; Capon, R. J. *Org. Biomol. Chem.* **2010**, *8*, 4682.
- (16) Sugiyama, R.; Nishimura, S.; Kakeya, H. *Tetrahedron Lett.* **2013**, *54*, 1531.
- (17) Sakanishi, K.; Itoh, S.; Sugiyama, R.; Nishimura, S.; Kakeya, H.; Iwabuchi, Y.; Kanoh, N. *Eur. J. Org. Chem.* **2014**, *2014*, 1376.
- (18) Sugiyama, R.; Nishimura, S.; Matsumori, N.; Tsunematsu, Y.; Hattori, A.; Kakeya, H. *J. Am. Chem. Soc.* **2014**, *136*, 5209.
- (19) (a) Zhang, W.; Li, S.; Zhu, Y.; Chen, Y. C.; Chen, Y.; Zhang, H.; Zhang, G.; Tian, X.; Pan, Y.; Zhang, S.; Zhang, W.; Zhang, C. *J. Nat. Prod.* **2014**, *77*, 388. (b) Zhu, Y.; Zhang, W.; Chen, Y.; Yuan, C.; Zhang, H.; Zhang, G.; Ma, L.; Zhang, Q.; Tian, X.; Zhang, S.; Zhang, C. *ChemBioChem* **2015**, *16*, 2086.
- (20) Rickards, R. W.; Smith, R. M.; Golding, B. T. *J. Antibiot.* **1970**, *23*, 603.
- (21) Kells, P. M.; Ouellet, H.; Santos-Aberturas, J.; Aparicio, J. F.; Podust, L. M. *Chem. Biol.* **2010**, *17*, 841.
- (22) We modeled this step and found it to be exergonic by 13.6 kcal mol<sup>-1</sup>. For details, see Supporting Information.
- (23) Frisch, M. J.; Trucks, G. W.; Schlegel, H. B.; Scuseria, G. E.; Robb, M. A.; Cheeseman, J. R.; Scalmani, G.; Barone, V.; Mennucci, B.; Petersson, G. A.; Nakatsuji, H.; Caricato, M.; Li, X.; Hratchian, H. P.; Izmaylov, A. F.; Bloino, J.; Zheng, G.; Sonnenberg, J. L.; Hada, M.; Ehara, M.; Toyota, K.; Fukuda, R.; Hasegawa, J.; Ishida, M.; Nakajima, T.; Honda, Y.; Kitao, O.; Nakai, H.; Vreven, T.; Montgomery, J. A., Jr.; Peralta, J. E.; Ogliaro, F.; Bearpark, M.; Heyd, J. J.; Brothers, E.; Kudin, K. N.; Staroverov, V. N.; Kobayashi, R.; Normand, J.; Raghavachari, K.; Rendell, A.; Burant, J. C.; Iyengar, S. S.; Tomasi, J.; Cossi, M.; Rega, N.; Millam, J. M.; Klene, M.; Knox, J. E.; Cross, J. B.; Bakken, V.; Adamo, C.; Jaramillo, J.; Gomperts, R.; Stratmann, R. E.; Yazyev, O.; Austin, A. J.; Cammi, R.; Pomelli, C.; Ochterski, J. W.; Martin, R. L.; Morokuma, K.; Zakrzewski, V. G.; Voth, G. A.; Salvador, P.; Dannenberg, J. J.; Dapprich, S.; Daniels, A. D.; Farkas, O.; Foresman, J. B.; Ortiz, J. V.; Cioslowski, J.; Fox, D. J. *Gaussian 09*, revision D.01; Gaussian, Inc.: Wallingford, CT, 2009.
- (24) (a) Becke, A. D. *J. Chem. Phys.* **1993**, *98*, 5648. (b) Lee, C.; Yang, W.; Parr, R. G. *Phys. Rev. B: Condens. Matter Mater. Phys.* **1988**, *37*, 785.
- (25) Grimme, S.; Antony, J.; Ehrlich, S.; Krieg, H. *J. Chem. Phys.* **2010**, *132*, 154104.
- (26) Zhao, Y.; Truhlar, D. G. *Phys. Chem. Chem. Phys.* **2008**, *10*, 2813.
- (27) (a) Zhao, Y.; Truhlar, D. G. *Theor. Chem. Acc.* **2008**, *120*, 215. (b) Zhao, Y.; Truhlar, D. G. *Acc. Chem. Res.* **2008**, *41*, 157.
- (28) Lan, Y.; Zou, L.-F.; Cao, Y.; Houk, K. N. *J. Phys. Chem. A* **2011**, *115*, 13906.
- (29) (a) Barone, V.; Cossi, M. *J. Phys. Chem. A* **1998**, *102*, 1995. (b) Cossi, M.; Rega, N.; Scalmani, G.; Barone, V. *J. Comput. Chem.* **2003**, *24*, 669. (c) Takano, Y.; Houk, K. N. *J. Chem. Theory Comput.* **2005**, *1*, 70.
- (30) Legault, C. Y. *CYLview*, version 1.0b; Université de Sherbrooke: Quebec, Canada, 2009; <http://www.cylview.org>.
- (31) Dennington, R.; Keith, T.; Millam, J. *GaussView*, version 5; Semichem Inc.: Shawnee Mission, KS, 2009.
- (32) (a) *Avogadro*: an open-source molecular builder and visualization tool, version 1.1.1; <http://avogadro.openmolecules.net/>. (b) Hanwell, M. D.; Curtis, D. E.; Lonie, D. C.; Vandermeersch, T.; Zurek, E.; Hutchison, G. R. *J. Cheminf.* **2012**, *4*, 17.
- (33) *MacroModel*, version 10.3, Schrödinger, LLC: New York, 2014.
- (34) Pham, H. V.; Houk, K. N. *J. Org. Chem.* **2014**, *79*, 8968.

- (35) (a) Caramella, P.; Quadrelli, P.; Toma, L. *J. Am. Chem. Soc.* **2002**, *124*, 1130. (b) Ess, D. H.; Wheeler, S. E.; Iafe, R. G.; Xu, L.; Çelebi-Ölçüm, N.; Houk, K. N. *Angew. Chem., Int. Ed.* **2008**, *47*, 7592. (c) Wang, Z.; Hirschi, J. S.; Singleton, D. A. *Angew. Chem., Int. Ed.* **2009**, *48*, 9156. (d) Wang, T.; Hoye, T. R. *Nat. Chem.* **2015**, *7*, 641.
- (36) Rehbein, J.; Carpenter, B. K. *Phys. Chem. Chem. Phys.* **2011**, *13*, 20906 and references therein.
- (37) Bofill, J. M.; Quapp, W. J. *Math. Chem.* **2013**, *51*, 1099.
- (38) Maeda, S.; Harabuchi, Y.; Ono, Y.; Taketsugu, T.; Morokuma, K. *Int. J. Quantum Chem.* **2015**, *115*, 258.
- (39) Thomas, J. B.; Waas, J. R.; Harmata, M.; Singleton, D. A. *J. Am. Chem. Soc.* **2008**, *130*, 14544.
- (40) The truncated model substrate **5t** and the two cycloadducts are shown below. For details, see [Supporting Information](#).



- (41) Hoffmann, R. W. *Chem. Rev.* **1989**, *89*, 1841.
- (42) Allinger, N. L.; Miller, M. A. *J. Am. Chem. Soc.* **1961**, *83*, 2145.